Nanoparticle-mediated cellular response is size-dependent

WEN JIANG[1,2], BETTY Y. S. KIM[1,2,3], JAMES T. RUTKA[3] AND WARREN C. W. CHAN[1,2]*

[1]Institute of Biomaterials and Biomedical Engineering, University of Toronto, 164 College Street, Toronto, Ontario M5S 3G9, Canada
[2]Terrence Donnelly Centre for Cellular & Biomolecular Research, University of Toronto, 160 College Street, Toronto, Ontario M5S 3E1, Canada
[3]Division of Neurosurgery, The Hospital for Sick Children, University of Toronto, 555 University Avenue, Toronto, Ontario M5G 1X8, Canada
*e-mail: warren.chan@utoronto.ca

Published online: 2 March 2008; doi:10.1038/nnano.2008.30

Nanostructures of different sizes, shapes and material properties have many applications in biomedical imaging, clinical diagnostics and therapeutics[1–6]. In spite of what has been achieved so far, a complete understanding of how cells interact with nanostructures of well-defined sizes, at the molecular level, remains poorly understood. Here we show that gold and silver nanoparticles coated with antibodies can regulate the process of membrane receptor internalization. The binding and activation of membrane receptors and subsequent protein expression strongly depend on nanoparticle size. Although all nanoparticles within the 2–100 nm size range were found to alter signalling processes essential for basic cell functions (including cell death)[7], 40- and 50-nm nanoparticles demonstrated the greatest effect. These results show that nanoparticles should no longer be viewed as simple carriers for biomedical applications, but can also play an active role in mediating biological effects. The findings presented here may assist in the design of nanoscale delivery and therapeutic systems and provide insights into nanotoxicity.

Cells control their function and state through numerous processes of intracellular signalling events that are normally triggered by the binding of a ligand molecule with cell surface receptors. The extent of receptor–ligand binding and receptor crosslinking affects the intensity and duration of intracellular signalling and other downstream events, such as those seen with the transmembrane receptor tyrosine kinases[8,9]. Ligands with multiple receptor binding sites, known as multivalent ligands, can crosslink the membrane receptors more efficiently to regulate signalling processes[10]. Nanoparticles coated with antibodies could potentially function as multivalent ligands that are capable of crosslinking surface receptors. By changing the size, shape and material properties of the engineered nanoparticles, the degree of receptor crosslinking and subsequent cell responses can be precisely controlled.

Recent observations in biological systems suggest that the physical parameters of nanoparticles can affect their nonspecific uptake in cells, with potential to induce cellular responses[11–13]. However, these studies provide limited information regarding the cellular processes involved in nanoparticle trafficking and their ensuing functional impact. The understanding of how engineered nanoparticles of different geometries interact with cells requires the study of the molecular events involved in nanoparticle–membrane receptor binding, endocytosis and subsequent signalling activation. The characterization of these molecular processes, which can provide novel means to modulate cellular behaviours, has not been explored. Furthermore, studies involving ligand-coated nanoparticles have added clinical significance, because the information provided can benefit the design of targeted therapeutic and diagnostic platforms. To demonstrate that engineered nanoparticles of well-defined sizes actively participate in the processes of regulating and modulating cellular responses, we synthesized multivalent engineered nanoparticles to selectively control specific interactions between Herceptin and its receptor ErbB2, a receptor tyrosine kinase overexpressed in various ovarian and breast cancers (Fig. 1a; see also Supplementary Information, Fig. S1)[14,15]. The attachment of multiple Herceptin molecules onto the nanoparticle surface allows the formation of multivalent engineered nanoparticles for crosslinking surface ErbB2 receptors and to alter cell fate.

To test this hypothesis, stable suspensions of nanostructures of varying multivalency were prepared using colloidal gold nanoparticles (GNPs) of sizes ranging from 2 to 100 nm (see Supplementary Information, Figs S2 and S3, Table S1)[16]. Despite a deficiency in covalent linkage, Herceptin–GNP complexes (Her–GNPs) exhibited relative stability in various conditions for the duration of the experiment (see Supplementary Information, Figs S4 and S5). As compared with unmodified GNPs, we observed a significant enhancement in the uptake of Her–GNPs when incubated with ErbB2 overexpressing human breast cancer SK-BR-3 cells (see Supplementary Information, Fig. S6). The internalization of Her–GNPs was highly dependent on temperature (Fig. 1b). The observed binding of Her–GNPs with the plasma membrane and sequestration within coated pits suggest that the minimal nanoparticle internalization at 4 °C incubation is likely due to mechanisms that are independent of receptor–ligand binding inhibition (Fig. 1b). On the other hand, the presence of Her–GNPs within endosomes and multivesicular bodies at higher temperature indicates that receptor-mediated uptake is the most probable mechanism for nanoparticle uptake (Fig. 1b)[17]. As similar temperature-dependent internalization patterns of ErbB2 receptors have been reported using antibody crosslinking[18], multivalent binding of Her–GNPs with ErbB2 receptors is probably the initiator of this uptake process. In addition, the internalization of Her–GNPs was highly dependent on size, with the most efficient uptake occurring within the 25–50 nm size range (see Supplementary Information, Fig. S7). The accumulation of Her–GNPs was particularly evident within

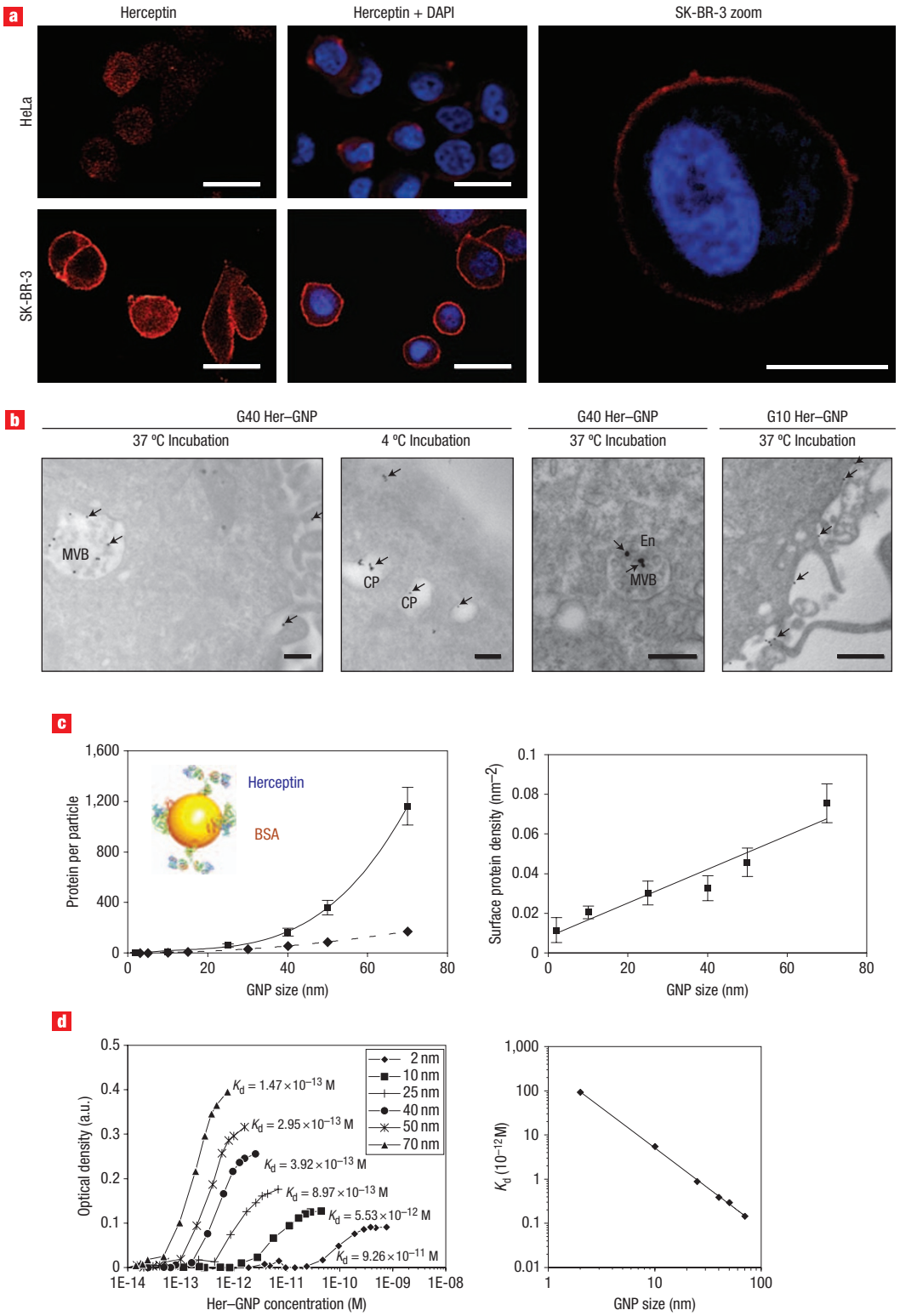

Figure 1 Specific interactions between Her–GNPs and ErbB2 receptors determine their internalization fate. a, Fluorescence images showing specific binding of Herceptin antibody (labelled with the Texas red dye molecule) to the ErbB2 receptors in SK-BR-3 cells. The cell nucleus is labelled with DAPI (blue). HeLa cells served as control. The enlarged view represents a single SK-BR-3 cell (scale bars = 5 μm). **b**, TEM images of cells incubated with G40 Her–GNPs at 37 °C and 4 °C and G40 and G10 Her–GNPs at 37 °C. Arrows indicate Her–GNPs (scale bars = 0.5 μm). MVB, multivesicular bodies; En, endosomes; CP, clathrin-coated pits. **c**, Antibody loading analysis. Left panel: Herceptin adsorption as a function of nanoparticle size (filled squares, experimental measurement; filled diamonds, calculation assuming constant Herceptin coverage area). Right panel: Surface-bound Herceptin density correlates with GNP size. Error bars, ±s.d.; $n = 6$. **d**, Binding avidity analysis. Left panel: Effect of dissociation constant K_d for different-sized Her–GNPs. Right panel: K_d is inversely proportional to GNP size.

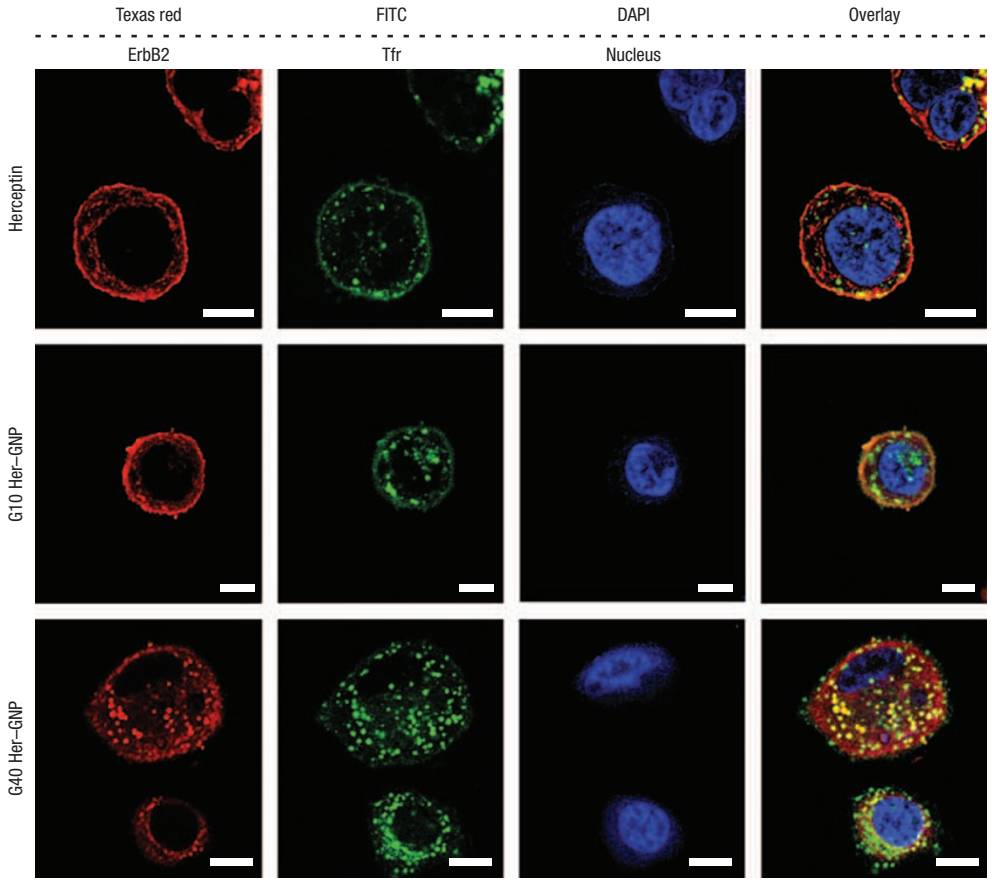

Figure 2 Dependence of ErbB2 receptor internalization on nanoparticle size. Laser confocal fluorescence microscopy of SK-BR-3 cells treated for 3 h with free Herceptin, and G10 and G40 Her–GNPs. Cells were then labelled with anti-ErbB2 (red) and anti-transferrin receptor (Tfr) antibodies (green), and the nucleus was counterstained with DAPI (blue). Co-localization of ErbB2 and Tfr was observed in cells treated with G40 Her–GNPs (yellow). Limited ErbB2 receptor internalization was observed for cells treated with free Herceptin and G10 Her–GNPs (scale bars = 10 μm).

subcellular organelles responsible for receptor degradation, including endosomes, multivesicular bodies and lysosomes. Considerable reduction in cellular uptake was observed for Her–GNPs outside this size range, with predominant localization on plasma membranes or protrusions (Fig. 1b).

To analyse the size-dependent internalization of Her–GNPs, we studied the binding dynamics between Her–GNPs and ErbB2 receptors. The number of allowable Herceptin binding sites on nanoparticles is dependent on the surface area, which increases with particle radius R (Fig. 1c). In addition, antibody density on the particle surface increases linearly with respect to R owing to the reduction in the average area covered by each protein (Fig. 1c). The higher surface curvature of smaller nanoparticles restricts the relative orientation between molecules with a certain degree of conformational rigidity and their docking surface during the adsorption process, resulting in large background areas without protein coverage[19]. Larger nanoparticles have a higher protein-to-nanoparticle ratio, which allows the restructuring of protein postures on the nanoparticle surface to maximize protein loading[20]. The overall increase in protein adsorption correlates with particle size (proportional to R^3), which significantly enhances the multivalency of Her–GNPs. Therefore, these multivalent antibody–nanoparticles exhibit a high degree of ErbB2 crosslinking capability, which is tunable by nanoparticle size.

Changes in nanoparticle size also affect the binding capacity of Her–GNPs with ErbB2 receptors. The dissociation constant K_d was shown to vary inversely with the size of Her–GNPs (Fig. 1d). Notably, 2-nm (G2) Her–GNPs were observed to have a similar K_d value as free Herceptin ($\sim 1 \times 10^{-10}$ M) (ref. 14), and 40-nm (G40) Her–GNPs had a K_d value of 4×10^{-13} M. Therefore, with higher binding avidity, larger Her–GNPs can firmly anchor on cell surfaces, resulting in prolonged receptor binding. Given that the internalization process is strongly dependent on the membrane wrapping time, which is based on the diffusion rate of receptors on the plasma membrane surface, extremely small or large nanoparticles would both yield inefficient uptake[11,21]. Combined with the inability to promote multivalent binding, smaller nanoparticles dissociate from the receptors before being engulfed by the membrane owing to low binding avidity. In contrast, despite their enhanced multivalent binding, extremely large nanoparticles possess a much higher antibody density on the particle surface. Thus, the inability to compensate for the depletion of receptors within the area of binding through global diffusive motion of distant receptors could limit the process of membrane wrapping that is necessary for nanoparticle internalization[21]. Our data suggests that 40- to 50-nm nanoparticles form the critical cutoff point for receptor-mediated internalization. Such an optimal size for particle uptake

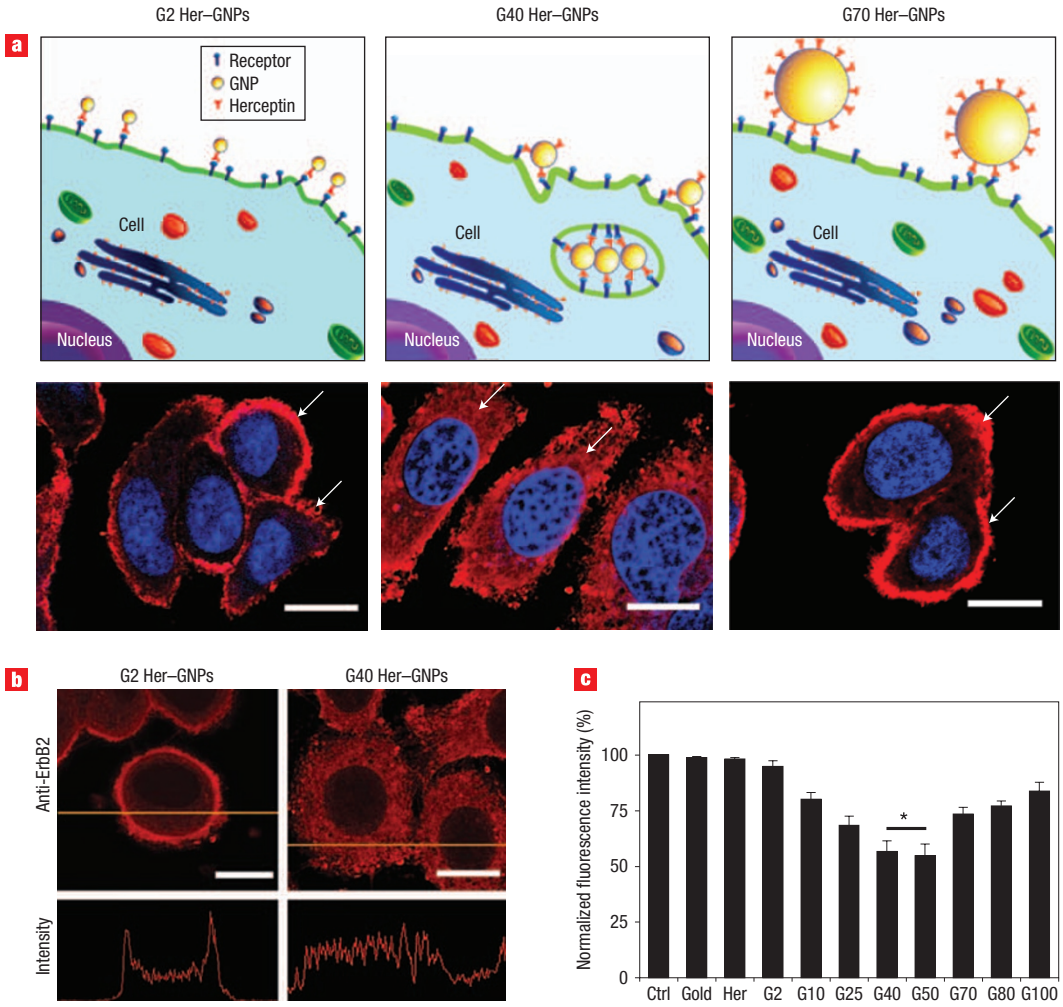

Figure 3 Dependence of downregulation of membrane ErbB2 expression on nanoparticle size. a, Illustrations with corresponding fluorescence images of ErbB2 receptor localization after treatment with different-sized Her–GNPs. Arrows indicate ErbB2 receptors, and the nucleus is counterstained with DAPI (blue) (scale bars=10 μm). **b**, Cross-sectional fluorescence intensity measurements of ErbB2 receptor localization patterns with G2 and G40 Her–GNPs (scale bars = 10 μm). **c**, Surface ErbB2 expression analysis using untreated cells normalized as 100% expression level (Ctrl). Cells were treated with unmodified 40-nm GNPs (Gold), Herceptin (Her) and Herceptin-modified GNPs of various sizes (* denotes statistical significance for G40/G50 compared to Her–GNPs of other sizes, $p < 0.05$, ANOVA). Error bars, ±s.d.; $n = 4$.

is probably due to the direct balance between multivalent crosslinking of membrane receptors and the process of membrane wrapping involved in receptor-mediated endocytosis.

To examine whether Her–GNPs and ErbB2 receptors are internalized as a unit complex, co-localization of ErbB2 and transferrin receptors, a protein with a well-documented receptor-mediated endocytosis pathway, was studied[22]. In cells treated with free Herceptin, ErbB2 receptors were localized primarily on the plasma membrane[23]. In contrast, the endosomal co-localization of ErbB2 and transferrin receptors with G40 Her–GNPs incubation suggests that the receptors do in fact undergo endocytosis when bound to Her–GNPs of a specific size regime (Fig. 2; see also Supplementary Information, Fig. S8). Although these receptors are normally internalization-impaired[24], these findings demonstrate that selective stimulation of receptor–ligand complex internalization through multivalent crosslinking can be achieved by controlling the size of Her–GNPs.

The endocytic process is a direct attenuation mechanism for membrane receptor presentation[25]. Downregulation of the membrane ErbB2 level was found to be modulated by means of Her–GNP-induced crosslinking. Cells treated with free Herceptin, G2, G10 and G70 Her–GNPs exhibited similar patterns of membrane ErbB2 localization, with little or no cytoplasmic presence (Figs 2 and 3). For G25 and G40 Her–GNP treated cells, a significant portion of ErbB2 receptors was found inside the cytoplasm (Fig. 3a). Cross-sectional analysis using fluorescence intensity profiling confirmed ErbB2 redistribution from the cell surface to the cytoplasm (Fig. 3b). This fluctuation in surface ErbB2 level was most significant in cells treated with G40/G50 Her–GNPs, with 40% reduction observed in both cases (Fig. 3c). A similar size-dependent trend in the reduction of membrane receptor presentation was also observed in other nanoparticle systems, including Herceptin-coated silver nanoparticles (Her–SNPs) (see Supplementary Information, Figs S9, S10, Table S2). Taken together, these results indicate that a universal route of membrane receptor downregulation can be achieved using nanoparticle size.

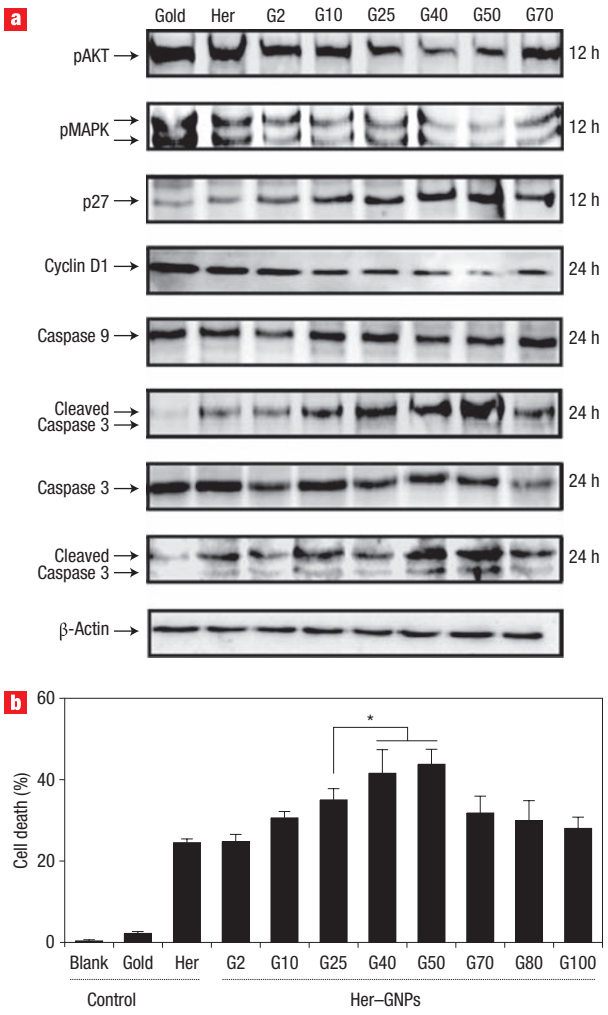

Figure 4 Influence of different-sized nanoparticles on downstream protein expression. a, Western blot of key intracellular signalling proteins that are involved in cellular proliferation and survival. β-Actin served as loading control. **b**, TUNEL analysis of apoptotic cells treated with unmodified 40-nm GNPs (Gold), free Herceptin (Her) and Herceptin-modified GNPs of various sizes. The percentage of cells that undergo apoptosis was more significant for cells treated with G40/G50 Her–GNPs as compared to Herceptin alone, or with other sizes of Her–GNPs ($p < 0.05$, * denotes $p < 0.1$, ANOVA followed by Student's *t*-test). Error bars, $\pm$s.d.; $n = 4$.

The altered membrane receptor presentation level in Her–GNP-treated cells directly influences the post-translational modification of the downstream kinases that are crucial for ErbB2 signalling[26]. A significant reduction in AKT and MAPK activation was observed, with the greatest effect observed in cells treated with G40/G50 Her–GNPs (Fig. 4a). Repressed expression of cell cycle regulators downstream of AKT, such as cyclin D1 was observed at 24 h, and cyclin-dependent kinase inhibitor p27 expression was elevated after 12 h of incubation. In contrast, the basal level of expression of these proteins in cells treated with free Herceptin suggests that Her–GNPs are actively involved in enhancing the growth inhibitory effects (Fig. 4a). Because AKT activation can also inhibit apoptotic signalling[7], we examined the role of caspase activation. Treatment of cells with G40 Her–GNPs showed increased caspase-9 and caspase-3 cleavage, with an almost twofold enhancement in cell death compared with Herceptin treatment alone (Fig. 4a). Although the induction of apoptotic activities was enhanced for all Her–GNPs, the greatest difference was observed in G40 or G50 Her–GNP-treated cells (Fig. 4b). Similar experimental outcomes were independently confirmed using Her–SNPs, indicating that the observed effects hold for other nanoparticle systems as well (see Supplementary Information, Fig. S11).

In summary, we have demonstrated that engineered nanoparticles of well-defined sizes can selectively induce membrane receptor internalization to downregulate their expression level. This in turn alters the downstream signalling and subsequent cellular responses. These findings provide strong evidence that nanostructures can not only passively interact with cells, but also actively engage and mediate the molecular processes that are essential for regulating cell functions. This concept, therefore, has significant implications in understanding the interactions of nanostructures with biological systems and assisting in the design of intelligent nanodevices, with great potential for the development of novel molecular-based diagnostics and therapeutics.

METHODS

CELL CULTURE

Human breast cancer SK-BR-3 cells (American Type Culture Collection) were maintained in McCoy's 5a medium modified with 1.5 mM L-glutamine (Invitrogen), supplemented with 10% fetal bovine serum (FBS) (Sigma) and 5% penicillin/streptomycin. SNB-19 and HeLa cells were cultured in Dulbecco's Modified Eagle's Medium (DMEM), supplemented with 10% FBS and 5% penicillin/streptomycin. Cell cultures were incubated at 37 °C and equilibrated in 4% CO_2 and air. Herceptin (Trastuzumab) was a generous gift supplied by Genentech.

NANOPARTICLE SYNTHESIS

Various sizes of GNPs were synthesized according to the method developed by Frens[27]. GNPs were used as a model system because of the simplicity and reproducibility of the synthetic and bioconjugation techniques. Briefly, 300 μl of 1% chloroauric acid (Sigma-Aldrich) was added to 30 ml of double-distilled water and the solution was heated to boiling. Next, 600 μl, 450 μl and 250 μl of 1% citric acid (Sigma-Aldrich) were added to the solution to synthesize 10-, 25- and 40-nm GNPs, respectively. The solution was refluxed until a colour change from dark blue to red was observed. Once cooled to room temperature, the solution was purified by centrifuging for 5 min at 6,000*g* and discarding the pellet. For GNPs smaller than 10 nm, we adopted the method of Bonnard *et al.*[28], in which sodium borohydride was used as the reducing agent. UV-Vis spectra of the various GNP solutions were recorded with the UV-1601PC spectrophotometer (Shimadzu) using 1-cm quartz cuvettes. For SNPs, 20-, 40-, 60- and 80-nm colloids were purchased from Ted Pella. Both 50- and 90-nm SNPs were obtained from Prof. G. Chumanov at Clemson University. Smaller silver nanoparticles (5- and 10-nm) were prepared according to the methods of Solomon *et al.*[29]. Briefly, 1.0 mM of silver nitrate (Sigma-Aldrich) was added in a dropwise fashion to 2.0 mM ice-cold sodium borohydride solution (Sigma-Aldrich). By varying the addition of silver nitrate, different sizes of SNPs were synthesized.

ErbB2 SURFACE EXPRESSION ANALYSIS

SK-BR-3 cells were treated with free 40-nm GNPs, free Herceptin and Herceptin-modified nanoparticles of different sizes for 3–4 h. For all treatment conditions the concentration of Herceptin (free and modified) was kept constant at 10 μg ml^{-1}. Cells were washed three times using PBS, blocked with 1% BSA, then incubated with mouse monoclonal anti-ErbB2 antibody (2 μg ml^{-1}) for 30 min at 37 °C. Once washed, cells were incubated with Alexa 488 conjugated goat anti-mouse IgG1 antibody (2 μg ml^{-1}) for 30 min and analysed using the Beckman-Coulter Epics XL flow cytometer. Similar procedures were followed for SNP studies.

IMMUNOFLUORESCENCE MICROSCOPY

Herceptin was conjugated to Texas red succinimidyl ester (Invitrogen) and purified using a size-exclusion Sephadex G-25 column (Sigma). Cells were

washed three times in PBS, fixed with ice-cold ethanol, then blocked using 1% BSA in PBS for 20 min. For ErbB2 detection, these cells were incubated with 2.5 μg ml^{-1} of Herceptin–Texas red conjugates for 30 min. Cells were washed repeatedly to remove the excess bioconjugates. The nucleus was counterstained with DAPI (Sigma). Fluorescence images were taken using a Zeiss LSM 510 confocal microscope with a 40× objective lens. For ErbB2 imaging, cells were treated with Herceptin-modified GNPs of various sizes for 3 h at 37 °C. These cells were then fixed with 4% paraformaldehyde fixative and permeabilized with ice-cold ethanol and blocked with 1% BSA. Cells were then incubated with mouse anti-ErbB2 receptor antibody and anti-transferrin receptor antibody for 30 min. Texas red/Alexa 488 conjugated goat anti-mouse IgG1 were added at a concentration of 5–10 μg ml^{-1}.

Received 3 October 2007; accepted 23 January 2008; published 2 March 2008.

References

1. Xia, Y. *et al*. One-dimensional nanostructures: Synthesis, characterization, and applications. *Adv. Mater.* **15,** 353–389 (2003).
2. Alivisatos, A. P. Semiconductor clusters, nanocrystals, and quantum dots. *Science* **271,** 933–937 (1996).
3. Elghanian, R., Storhoff, J. J., Mucic, R. C., Letsinger, R. L. & Mirkin, C. A. Selective colorimetric detection of polynucleotides based on the distance-dependent optical properties of gold nanoparticles. *Science* **227,** 1078–1081 (1997).
4. Cao, Y. C., Jin, R. & Mirkin, C. A. Nanoparticles with Raman spectroscopic fingerprints for DNA and RNA detection. *Science* **297,** 1536–1540 (2002).
5. Klostranec, J. & Chan, W. C. W. Quantum dots in biological and biomedical research: recent progress and present challenges. *Adv. Mater.* **18,** 1953–1964 (2006).
6. Hirsch, L. R. *et al*. Nanoshell-mediated near-infrared thermal therapy of tumors under magnetic resonance guidance. *Proc. Natl Acad. Sci. USA* **100,** 13549–13554 (2003).
7. Datta, S. R., Brunet, A. & Greenberg, M. E. Cellular survival: a play in three Akts. *Genes Dev.* **13,** 2905–2927 (1999).
8. Ullrich, A. & Schlessinger, J. Signal transduction by receptors with tyrosine kinase activity. *Cell* **61,** 203–212 (1990).
9. Schlessinger, J. Cell signaling by receptor tyrosine kinases. *Cell* **103,** 211–225 (2000).
10. Dubois, P. M., Stepinski, J., Urbain, J. & Sibley, C. H. Role of the transmembrane and cytoplasmic domains of surface IgM in endocytosis and signal transduction. *Eur. J. Immunol.* **22,** 851–857 (1992).
11. Chithrani, B. D., Ghazani, A. A. & Chan, W. C. W. Determining the size and shape dependence of gold nanoparticle uptake into mammalian cells. *Nano Lett.* **6,** 662–668 (2006).
12. Osaki, F., Kanamori, T., Sando, S., Sera, T. & Aoyama, Y. A quantum dot conjugated sugar ball and its cellular uptake. On the size effects of endocytosis in the subviral region. *J. Am. Chem. Soc.* **126,** 6520–6521 (2004).
13. Shortkroff, S., Turell, M., Rice, K. & Thornhill T. S. Cellular response to nanoparticles. *Mater. Res. Soc. Symp. Proc.* **704,** W11.5.1–W11.5.6 (2002).
14. Carter, P. *et al*. Humanization of an anti-p185^{HER2} antibody for human cancer therapy. *Proc. Natl Acad. Sci. USA* **89,** 4285–4289 (1992).
15. Rubin, L. & Yarden, Y. The basic biology of Her2. *Ann. Oncol.* **12,** S3–S8 (2001).
16. Geoghegan, W. D. & Ackerman, G. A. Adsorption of horseradish peroxidase, ovomucoid and anti-immunoglobulin to colloidal gold for the indirect detection of concanavalin A, wheat germ agglutinin and goat anti-human immunoglobulin G on cell surfaces at the electron microscopic level: a new method, theory and application. *J. Histochem. Cytochem.* **25,** 1187–1200 (1977).
17. Chithrani, D. B. & Chan, W. C. W. Elucidating the mechanism of cellular uptake and removal of protein-coated gold nanoparticles of different sizes and shapes. *Nano Lett.* **7,** 1542–1550 (2007).
18. Hommelgaard, A. M., Lerdrup, M. & van Deurs, B. Association with membrane protrusions makes ErbB2 an internalization-resistant receptor. *Mol. Biol. Cell* **15,** 1557–1567 (2004).
19. Ghitescu, L. & Bendayan, M. Immunolabeling efficiency of protein A–gold complexes. *J. Histochem. Cytochem.* **38,** 1523–1530 (1990).
20. Horrisberger, M. & Clerk, M. F. Labeling of colloidal gold with protein A. A quantitative study. *Histochemistry* **82,** 219–223 (1985).
21. Gao, H., Shi, W. & Freund, L. B. Mechanics of receptor-mediated endocytosis. *Proc. Natl Acad. Sci. USA* **102,** 9469–9474 (2005).
22. Andrews, N. C. Iron homeostasis: Insights from genetics and animal models. *Nat. Rev. Genet.* **1,** 208–217 (2000).
23. Austin, C. D. *et al*. Endocytosis and sorting of ErbB2 and the site of action of cancer therapeutics Trastuzumab and Geldanamycin. *Mol. Biol. Cell* **15,** 5268–5282 (2004).
24. Baulida, J., Kraus, M. H., Alimandi, M., Di Fiore, P. P. & Carpenter, G. All ErbB receptors other than the epidermal growth factor receptor are endocytosis impaired. *J. Biol. Chem.* **271,** 5251–5257 (1996).
25. Vieira, A. V., Lamaze, C. & Schmid, S. L. Control of EGF receptor signaling by clathrin-mediated endocytosis. *Science* **274,** 2086–2089 (1996).
26. Yakes, F. M. *et al*. Herceptin-induced inhibition of phosphatidylinositol-3 kinase and Akt is required for antibody-mediated effects on 27, Cyclin D1, and antitumour action. *Cancer Res.* **62,** 4132–4141 (2002).
27. Frens, G. Controlled nucleation for the regulation of the particle size in monodisperse gold suspensions. *Nature* **241,** 20–22 (1973).
28. Bonnard, C., Papermaster, D. S. & Kiraehenbuhl, J. P. The streptavidin–biotin bridge technique: Applications in light and electron microscope immunocytochemistry, in *Immunolabeling for Electron Microscopy*, 95–111 (Elsevier, New York, 1984).
29. Solomon, S. D., Bahadory, M., Jeyarajasingam, A. V., Rutkowsky, S. A. & Boritz, C. Synthesis and study of silver nanoparticles. *J. Chem. Educ.* **84,** 322–325 (2007).

Acknowledgements

Financial support was provided by the Canadian Institutes of Health Research (W.C.W.C. and J.T.R.), Natural Sciences and Engineering Council of Canada (W.J., B.Y.S.K. and W.C.W.C.), Canadian Foundation for Innovation and Ontario Innovation Trust (W.C.W.C.), the Surgeon Scientist Program and the Ontario Ministry of Health (B.Y.S.K.). The authors wish to thank J. Klonstranec for helpful discussions, A. Manseur and T. Jennings for help with flow cytometry, B. Calvieri, S. Doyle and D. Holmyard with cell preparation for electron microscopy, and J. Oreopoulos from the Yip lab with confocal microscopy.

Correspondence and requests for materials should be addressed to W.C.W.C.

Supplementary Information accompanies this paper on www.nature.com/naturenanotechnology.

Author contributions

W.J., B.Y.S.K. and W.C.W.C designed the experiments. W.J. and B.Y.S.K. performed the experiments and gathered the data. All authors discussed the results, co-wrote the paper and commented on the manuscript. W.J. and B.Y.S.K. contributed equally to this work.